A WINDSHEAR HAZARD INDEX

Fred H. Proctor and David A. Hinton
NASA Langley Research Center
Hampton Virginia 23681-2199

and

Roland L. Bowles
AeroTech Research, Inc.
Hampton, Virginia 23666

Paper: 7.7, pages 482-487
Preprints of 9th Conference on Aviation, Range and Aerospace Meteorology
11-15 September 2000, Orlando Florida
American Meteorology Society

7.7 A WINDSHEAR HAZARD INDEX

Fred H. Proctor* and David A. Hinton
NASA Langley Research Center, Hampton Virginia
and
Roland L. Bowles
AeroTech Research, Inc., Hampton, Virginia

1. INTRODUCTION

An aircraft exposed to hazardous low-level windshear may suffer a critical loss of airspeed and altitude, thus endangering its ability to remain airborne. In order to characterize this hazard, a nondimensional index was developed based on aerodynamic principals and understanding of windshear phenomena. This paper reviews the development and application of the Bowles F-factor, which is now used by onboard sensors for the detection of hazardous windshear. It was developed and tested during NASA/FAA's airborne windshear program and is now required for FAA certification of onboard radar windshear detection systems. Reviewed in this paper are: 1) definition of windshear and description of atmospheric phenomena that may cause hazardous windshear, 2) derivation and discussion of the F-factor, 3) development of the F-factor hazard threshold, 4) its testing during field deployments, and 5) its use in accident reconstructions.

2. DEFINITION OF WINDSHEAR

In the context of aviation science, windshear refers to a wind speed or direction change experienced by an airplane over a particular distance or length of time. This definition covers an extremely wide range of meteorological phenomena, including convective turbulence, gust fronts, microburst, internal gravity waves, vertical shear (such as due to low-level atmospheric jetstreams), and terrain-influenced flow. Some of these events are merely nuisances, leading to poor ride quality, increased pilot workload, and rough landings. However, an aircraft exposed to windshear of sufficient intensity and duration, may lose flight performance with a critical reduction of airspeed or flight altitude. Windshear is deemed hazardous when it has the potential to reduce an aircraft's energy state at a rate faster than can be added back by engine thrust, and thus endangering the aircraft by either reducing its airspeed below stall speed or by diminishing its elevation above the ground. This danger is limited to departing and arriving aircraft, since at this phase of flight, aircraft carry minimal excess energy and are at low altitude and airspeed. Moreover, the danger at low altitudes is further enhanced by the aircraft's flight configuration of landing gear and flap settings, which require time to reconfigure in order to gain maximum performance.

3. WINDSHEAR HAZARD INDEX

An index that quantifies the windshear threat was developed by Bowles (1990a, 1990b), based on the fundamentals of flight mechanics and the current understanding of windshear phenomena. This index, known as the F-factor, incorporates observable atmospheric parameters, and scales with aircraft flight performance in such a way as to predict impending flight path deterioration.

The concept employed in the derivation of the F-factor is the total aircraft energy and its rate of change. The total aircraft energy is simply the sum of the air-mass relative kinetic energy (airspeed) and the internal potential energy (altitude above the ground). The aircraft total specific energy (energy per unit weight) is defined as $E_T = z + \frac{1}{2}\frac{V_a^2}{g}$, where V_a is airspeed, g is gravitational acceleration, and z is altitude above ground. The above relationship uses air-mass kinetic energy, since airspeed, not ground speed, describes an airplane's ability to climb and maintain altitude. Likewise, potential inertial energy is used since altitude above the ground is most important to an airplane and can be traded for increased airspeed. The time rate of change of E_T (which is also the potential rate of climb of the aircraft), can be equated with the aircraft energy input from thrust and drag, as:

$$\dot{E}_T = \dot{z} + \frac{V_a}{g}\dot{V}_a = V_a \frac{(T_r - D)}{W} \qquad (1)$$

where $(T_r - D) / W$ is the ratio of the aircraft thrust minus drag to weight; i.e. the excess thrust to weight capability of the aircraft. Note that when thrust equals drag the aircraft will maintain a constant speed and altitude, or the pilot may maneuver to exchange aircraft potential energy for kinetic energy. The above relationship is valid for a uniform airmass only. The effect of variable atmospheric wind fields can be included by combining *Eq.* (1) with the appropriate aircraft equations of motion (e.g., Frost and Bowles 1984). Neglecting second-order terms, the new relationship becomes:

* *Corresponding author address:* Fred H. Proctor, Airborne Systems Competency, NASA Langley Research Center, MS 156A, Hampton VA 23681-2199, email: f.h.proctor@larc.nasa.gov

$$\dot{E}_T = \dot{z} + \frac{V_a}{g}\dot{V}_a = V_a\left[\frac{T_r - D}{W} - \frac{\dot{U}_x}{g} + \frac{\dot{w}}{V_a}\right]$$
$$= V_a\left[\frac{T_r - D}{W} - F\right]$$

(2)

where U_x is the component of atmospheric wind directed horizontally along the flight path (positive for tail wind); $\dot{U}_x$ is the shear term – the time rate of change of U_x experienced by the aircraft, and w is the updraft within the airmass. In *Eq.* (2), the wind-field terms constitute a nondimensional parameter defined by Bowles (1990a, 1990b) as the *F-factor*:

$$F \equiv \frac{\dot{U}_x}{g} - \frac{w}{V_a} \qquad (3)$$

Note from *Eq.* (2) that a positive F-factor acts to decrease the energy state of an aircraft; the F-factor is positive for a descending air mass ($w < 0$) and a wind field accelerating in the direction of the flight path ($\dot{U}_x > 0$). In the absence of airmass vertical motion, performance-decreasing shears ($\dot{U}_x > 0$) act to decrease the energy state of the aircraft, while performance increasing shear ($\dot{U}_x < 0$) act to increase the energy state.

The shear term in *Eqs.* (2) and (3) is a function both of the meteorological event and the aircraft trajectory, e.g.,

$$\dot{U}_x = \frac{\partial U_x}{\partial x}\dot{x} + \frac{\partial U_x}{\partial z}\dot{z} + \frac{\partial U_x}{\partial t} \qquad (4)$$

Both horizontal and vertical shears contribute to the shear term. The first term in *Eq.* (4) is the product of the horizontal shear directed along the flight path and the aircraft ground speed. This term is the primary contributor to aircraft performance loss during most accident encounters. The second term is the product of the vertical change of horizontal wind and the aircraft ascent rate. This term predominates when the aircraft climbs or descends through strong vertical shears, but has no contribution for level flight. The final term is the local rate-of-change of horizontal wind with time, which usually has only secondary importance during typical windshear encounters. Rearranging terms in *Eq.* (2), the change in airspeed is:

$$\dot{V}_a = g\left[\frac{T_r - D}{W} - \frac{\dot{z}}{V_a} - F\right]$$

(5)

Note that a loss of airspeed in a performance-decreasing shear (with $F > 0$) can be minimized by an increase in thrust and a reduction in altitude. For a strong shear that exceeds the thrust capability of the aircraft, i.e., $F > (T_r - D)/W$, a pilot may either manage his flight so as to maintain altitude while decelerating, maintain airspeed while descending, or some compromise of the two. At low altitude during takeoff or landing, the speed margin above aerodynamic stall speed is minimal and the height is critical. Numerous studies have been conducted (e.g., Hinton 1990, 1992) on optimal and practical techniques for escaping a windshear encounter. The recommended procedure in use today (Federal Aviation Administration 1987) results in extracting the maximum performance from the aircraft and maximizing the likelihood of exiting the windshear event prior to stalling or making ground contact.

The excess thrust-to-weight capability varies with aircraft type. For a *4*-engine jet aircraft, the ratio may be about *0.15* at full thrust and maximum takeoff weight. Due to the thrust requirements for engine-out climb performance, *3*- and *2*-engined aircraft have higher performance than *4*-engine aircraft. A typical *3*-engine jet transport may have an excess thrust to weight ratio of *0.18* or more, while a twin-engine may exceed 0.2. Hence, by applying excess thrust, jet aircraft are capable of maintaining their energy state for conditions with F < 0.15. The situation becomes more critical for an unexpected windshear encounter on landing approach. The excess thrust to weight ratio is about *-0.05* for a typical approach on a *3-degree* glide slope. Hence, additional time would be needed to bring the aircraft to full thrust during a windshear encounter. Upon an unexpected encounter, significant total energy can be lost from the aircraft during the *5* to *10* seconds of time required to recognize the threat and reach full thrust (Hinton 1992).

Typical piston-engine general-aviation aircraft can reach full thrust in a shorter time than jet aircraft. As is apparent from *Eqs.* (2)-(4), the slower airspeed of piston aircraft reduces the impact from horizontal and vertical shear, but increases the significance of vertical winds. Hence, an atmospheric event considered hazardous to commercial jet aircraft may not be so for a piston-driven aircraft, and *vice versa.*

4. HAZARD THRESHOLDS

Since *Eqs.* (2)-(5) only describe the instantaneous effect of shear on aircraft specific energy and airspeed, the equations must be integrated over an appropriate scale length to characterize the hazard of the event. For example, very large magnitudes of *F* may occur for brief moments from turbulence associated with the convective planetary boundary layer, but the positive values of *F* are over small length scales and are quickly followed by negative values. Such oscillations of F-factor result in perceived turbulence, with airspeed oscillations and little net trajectory change. Thus, in order for the F-factor to be useful as a hazard metric it must be averaged or computed in such a way, to represent a significant deterioration in flight path. Such an effort was conducted by Lewis *et al* (1994). They proposed that the F-factor be averaged over some given horizontal extent (*L*) as:

$$\overline{F}(L) = \frac{1}{L}\int_x^{x+L} F\,ds = \frac{1}{L}\int_x^{x+L}\left(\frac{T_r - D}{W}\right)ds - \frac{\Delta V_a^2}{2gL} - \frac{\Delta Z}{L} \qquad (7)$$

where the right side of *Eq.* (7) relates an average F-factor to the airplane performance capability lost over the spatial extent *L*. From (7) it is possible to determine the magnitude and spatial extent that the aircraft can survive, given specific initial energy conditions (speed and height) and allowable energy loss. Calculations were performed by Lewis *et al* for a range of cases in order to identify a minimum hazard threshold for $\overline{F}$ and an appropriate minimum length scale (L) for windshear exposure. Each calculation assumed a profile of $(T_r - D)/W$ for a specific aircraft type on approach or departure. Each profile began with a value appropriate for either the take-off or landing phase of

flight (maximum for the airplane for takeoff and *-0.05* for landing approach), then a delay interval for pilot recognition of the shear (thrust does not change), followed by a thrust ramp up period (the excess thrust to weight ratio linearly increases to the maximum value). The pilot recognition delay period was assumed to begin at entry into the shear, and maximum $(T_r - D)/W$ was reached at the time indicated by the sum of the pilot delay and the engine spool up. This calculation was done for a number of airplane types representing a range of conventional jet transport aircraft, and was based on realistic but conservative data. The limiting case, representing a worst-case low-altitude encounter, required a *1-km* length scale and an average *F* of *0.12* or greater. The Federal Aviation Administration (FAA) has adopted the *1-km* average F-factor as its hazard metric for windshear detection systems on jet transports, and considers windshear hazardous for $\overline{F} > 0.1$, and a *must alert* threshold at *0.13* (e.g., Hinton 1994).

The study by *Lewis et al* (1994), however, did not address piston-driven aircraft, which composes the vast majority of general aviation aircraft. The minimum averaging scale and hazard threshold are yet to be determined for these types of aircraft.

4.1 Altitude Bound for Windshear Threat

Based on our current understanding of potential worst-case shears, the hazard from windshear is limited to elevations below *500 m*. For an unexpected windshear encounter above this altitude, a jet aircraft has an excess of potential energy that can be used to maintain flight speed (e.g., *Eq.* 5). In addition, an aircraft at this altitude is likely to have its landing gear up (increasing the level of maximum excess thrust), and may be carrying a larger airspeed.

4.2 Significance of Vertical Shear

Contribution of aircraft performance loss from vertical shear of horizontal wind can be evaluated from *Eqs.* (2)-(4). Any potential threat from vertical shear needs only to be evaluated for landing aircraft ($\dot{z} < 0$) when $\partial U_x/\partial z < 0$. Otherwise, for $\partial U_x/\partial z > 0$, a landing aircraft would encounter performance increasing shear; and for departing aircraft, any potential threat from vertical shear would be minimized by a flattening of the flight path angle (thus lessening the effect of the shear).

Assuming a hazard threshold of $\overline{F} = 0.1$, with *L=1000 m*, and using *Eqs.* (3) and (4), the vertical shear is hazardous to an aircraft on approach, if it exceeds:

$$\frac{\overline{\partial U_x}}{\partial z} > \frac{0.1g}{V_a \sin\gamma} \qquad (8)$$

In *Eq.* (8), the left hand term represents the average vertical shear of U_x over a depth of $L \sin\gamma$, where γ is the flight path angle. Assuming a typical approach speed of *75 m/s* and a flight path angle of *-6 degrees* (twice that of normal), the headwind would have to increase (with z) by at least *12.5 m* s^{-1} within a *100 m* thick layer in order to meet the above hazard criteria. Headwinds of this magnitude are unusual on arrival, and none of the major jetliner accidents has been attributed solely to vertical shear.

4.3 Implementation

Reactive, or in-situ systems utilize data from the aircraft's inertial/navigation and air data systems (Oseguera *et al* 1992). Reactive systems must rely on real-time calculations of F-factor and apply gust rejection filters to minimize nuisance alerts. These systems give accurate readings, but cannot give warnings until the windshear event has been penetrated. Computation of a 1-km average F-factor requires about 15 seconds of exposure at typical jet airplane approach speeds. Many commercial jet aircraft are now equipped with reactive windshear warning systems which employ the F-factor concept.

Forward-looking onboard windshear systems can predict an impending hazard along the aircraft's flight path (Arbuckle *et al* 1996). Most of these systems can sense the horizontal shear and its scale, but must rely on some estimation for vertical velocity. Furthermore, radar windshear systems require the presence of precipitation and adequate clutter suppression. Lidar systems must be concerned with attenuation due to water vapor and heavy precipitation.

5. ATMOSPHERIC WINDSHEAR PHENOMONA

The threat from low-altitude windshear is limited to those atmospheric phenomena that maintain a significant level of shear over a particular range of scales. Phenomena with high levels of *F*, but over short distances (horizontal scales less than *400 m*), are experienced as turbulence by commercial jet aircraft. Phenomena with wind shear distributed over large length scales (of order 10 km and greater) are unlikely to have magnitudes of shear that would directly affect the safety of an aircraft. However, those events having a mid-range of scales, *i.e.* horizontal scales of approximately *400* to *4000 m*, are most likely to impact the performance of departing and arriving aircraft. The primary atmospheric phenomenon that can produce hazardous low-altitude windshear within this range of scales is the microburst. Since the late 1970's when microburst phenomena were first recognized as threat to aviation (e.g., Fujita and Byers 1977), the vast majority of windshear accidents and incidents involving jet transports have been attributed to microbursts.

Strong low-level jets (LLJ) are sometimes associated with large magnitudes of vertical shear, although rarely reaching intensities hazardous to aircraft. The maximum wind speed of a LLJ is usually located at an altitude between *200* to *600 m* above ground level, with peak speed ranging from *10* to *21 m/s* (Whiteman *et al* 1997). The performance loss due to descent through a LLJ can be demonstrated with *Eqs.* (3) and (4). For example, if a LLJ has a *21 m/s* peak velocity at *200 m* AGL with winds decreasing to zero at the ground, then a typical approach into the headwind of the LLJ would generate an average F-factor (along a *3.8 km* path) of *0.042*. Hence, the performance loss experienced by a landing aircraft could be easily balanced by added thrust. Given the same example and using *Eq.* (8), the vertical shear only becomes hazardous if the aircraft descends along a *–7.2* degree flight path angle. Thus our analysis suggest that the vertical shear associated with low-level jetstreams is well within the performance capability of aircraft, although aircraft with limited excess-thrust capability should apply caution during extreme LLJ events and avoid unusually-steep landing approaches.

6. MICROBURSTS AND MACROBURSTS

A microburst is loosely defined as an intense local downdraft with divergent surface outflow. Microbursts are associated with precipitation from convective clouds, and may produce magnitudes of vertical velocity and horizontal shear that can threaten landing and departing aircraft. Radar meteorologists identify surface outflows as microburst when their peak horizontal divergence exceeds *10 m/s* within a *1-4 km* segment (e.g. Wilson *et al* 1984). Divergent outflows with horizontal scale greater than *4 km* are sometimes termed macrobursts (Fujita 1985), although they may contain one or more embedded microbursts. The F-factor is most hazardous near the center of microburst outflows due to the strong downward motion and divergent shear. Performance enhancing areas ($F<0$), which often surround the hazard area, are due to the increasing headwind and updraft near the edge of the outflow (e.g., Proctor and Bowles 1992, Bracalente *et al* 1994). The computed 1-km F-factor from the Delta L-1011 flight data recorder (FDR) data of the 1985 Dallas-Ft. Worth accident is shown in *Fig. 1*. The aircraft encountered a microburst on approach and crashed about *2000 m* short of the runway (Fujita 1986, Proctor 1988a, 1988b). The figure indicates that aircraft first encountered performance-enhancing shear at the edge of the microburst followed by hazardous values of $\overline{F}$ in excess *0.25* just prior to impact. The performance decreasing windshear of this event exceeded the aircraft's ability to generate thrust and robbed the aircraft of its ability to stay airborne.

Not all microburst may achieve intensities that are a hazard to commercial aviation. From a *251* microburst sample, Bowles (1990a) points out that approximately half would not qualify as a threat, as based on an hazard threshold for average F-factor of *0.1 (see Fig. 2)*. Values for $\overline{F}$ from microburst accident encounters range from about *0.2* to *0.36* (Targ and Bowles 1988, Proctor *et al* 1995). The magnitude of these values exceeds the performance capability of most aircraft, and indicates the severity of the windshear threat from *intense* microburst.

Proctor and Bowles (1992) found that the F-factor in microburst usually varied weakly with altitude, even though the contribution from horizontal shear diminishes with increasing altitude. Numerical model simulations indicate that the contribution from the horizontal component dominates near the ground but becomes less than the vertical component at altitude above about *200 m* (Byrd *et al* 1990). Since look-ahead sensor can only measure the component along the flight path, various models have been evaluated for estimating the vertical wind component of the F-factor (Vicroy 1992, 1994). The results of these studies show that within the altitude of greatest interest (below *300 m*) the following simple relationship worked very well:

$$F = F_h\left(1+\frac{\beta\, gz}{V_a^2}\right) \qquad (9)$$

where the horizontal contribution from *Eq.* (3) is defined as:

$$F_h = \frac{\dot{U}_x}{g} \cong \frac{V_a}{g}\frac{\partial u_x}{\partial x}$$

In *Eq.* (9), $\beta = 2$ if $F_h > 0$ and $\beta = 1$ if $F_h < 0$. Using the above approximations, an estimate of the total 1-km average F-factor can be deduced from the horizontal shear sensed by a look-ahead system. The estimated 1 km average *F* using *Eq.* (9) is compared in *Fig. 1* for the DFW accident case.

7. FLIGHT TESTS

During 1991 and 1992 extensive flight test were conducted within microburst environments at Denver and Orlando. More than 75 microburst and strong gust fronts were penetrated at low altitudes (*225-335 m*) by NASA's B-737 research aircraft (Arbuckle *et al* 1996). The plane was equipped with in situ, Doppler radar, Lidar, and infrared windshear detection systems. Windshear information also was uplinked from a prototype Terminal Doppler Weather Radar (TDWR) and was used to locate microburst events for potential encounters. The onboard look-ahead systems were activated prior to windshear encounters, and the aircraft in-situ system gathered "truth" data as the event was penetrated. The X-band onboard Doppler radar, which utilized clutter suppression algorithms and F-factor estimations based on *Eq.* (9), was found to work extremely well within both high-reflectivity (wet) and low-reflectivity (dry) microburst environments. A comparison of the radar estimated average F-factor and in situ F-factor are shown in *Fig. 3*. A comparison of TDWR estimated F-factor with in situ F-factor measured during the microburst penetrations is shown in *Fig. 4*.

8. ACCIDENT RECONSTRUCTION

A USAir DC-9 unexpectedly encountered a rapidly intensifying microburst on approach to Charlotte in July of 1994. The plane crashed after encountering hazardous windshear with $\overline{F}$ of about 0.3. The event was reconstructed using the aircraft flight profiles and a numerical simulation of the event with the Terminal Area Simulation System (TASS) model (see Proctor *et al* 1995). Analysis of the 1-km F-factor from the FDR data is shown with the TASS data in *Fig. 5*. A simulation of NASA's windshear radar was performed with ground clutter data, NASA's processing algorithms (including the estimation for vertical F-factor), and the three-dimensional TASS data set. In spite of the ground clutter, the radar simulation was able to identify the microburst hazard (*Fig. 6*) and issue a warning more than *30 s* prior to the encounter. This study suggests that if the airplane had been equipped with windshear radar the accident may have been avoided.

9. CONCLUDING REMARKS

Windshear hazard characterization was a major component of the NASA/FAA airborne windshear program. Windshear radar systems which utilize the F-factor hazard metric are being produced by private vendors. These systems are being certified by the FAA for installation on many new jet aircraft.

References

Arbuckle, P.D., M.S. Lewis, and D.A. Hinton, 1996: Airborne systems technology application to the windshear threat, 20th Congress of the International Council of the Aeronautical Sciences, ICAS Paper No. 96-5.7.1, pp. 1640-1650.

Bowles, R.L., 1990a: Reducing windshear risk through airborne systems technology. The 17th Congress of the ICAS, Stockholm, Sweden, 27 pp.

Bowles, R.L., 1990b: Windshear detection and avoidance – airborne systems survey. 29th IEEE Conf. on Decision and Control, Vol. 2, 708-736.

Bracalente, E.M., S.D. Harrah, P.R. Schaffner, and C.L. Britt 1994: NASA's airborne Doppler radar for detection of hazardous wind shear: Flight results. *Airborne Windshear Detection and Warning Systems. 1994. Fifth and Final Combined Manufacturers' and Technologists' Conference*, NASA CP-10139, DOT/FAA/RD-94/14-1, 82-102.

Byrd, G.P., F.H. Proctor, and R.L. Bowles, 1990: Evaluation of a technique to quantify microburst windshear hazard potential to aircraft. 29th IEEE Conf. on Decision and Control, Vol. 2, 689-695.

Federal Aviation Administration, 1987: *Wind Shear Training Aid.* (Available from NTIS as PB88-127196).

Frost, W., R.L. Bowles, 1984: Wind shear terms in the equations of aircraft motion. *J. Aircraft,* ***21,*** 866-872.

Fujita, T.T., H.R. Byers, 1977: Spearhead echo and downburst in the crash of an airliner. *Mon. Wea. Rev.,* ***105****,* 129-146.

Fujita, T.T., 1985: *The Downburst, Microburst and Macroburst.* University of Chicago Press, 122 pp.

Fujita, T.T., 1986: *DFW Microburst on August 2, 1985.* University of Chicago Press, 154 pp.

Hinton, D.A., 1990: Relative merits of reactive and forward-look detection for wind shear encounters during landing approach for various microburst escape strategies. NASA TM-4158, DOT/FAA/DS-89/35.

Hinton, D.A., 1992: Forward-look wind shear detection for microburst recovery. *J Aircraft,* ***29***, 63-66.

Hinton, D.A., 1993: Airborne derivation of microburst alerts from ground-based Terminal Doppler Weather Radar Information – A flight evaluation. NASA TM-108990, 29 pp.

Hinton, D.A., 1994: Flight test evaluation of a data link and aircraft integration of TDWR wind-shear information. *Airborne Windshear Detection and Warning Systems. 1994. Fifth and Final Combined Manufacturers' and Technologists' Conference*, NASA CP-10139, DOT/FAA/RD-94/14-1, 23-48.

Lewis, M.S., P.A. Robinson, D.A. Hinton, and R.L. Bowles, 1994: The relationship of an integral wind shear hazard to aircraft performance limitations. NASA TM-109080.

Oseguera, R.M., R.L. Bowles, and P.A. Robinson, 1992: Airborne in situ computation of the wind shear hazard index. AIAA 92-0291.

Proctor, F.H., 1988a: Numerical simulations of an isolated microburst. Part I: dynamics and structure. *J. Atmos. Sci.,* ***45****,* 3137-3160.

Proctor, F.H., 1988b: Numerical simulation of the 2 August 1985 DFW microburst with the three-dimensional Terminal Area Simulation System. Preprints Joint Session of 15th Conf. on Severe Local Storms and Eighth Conf. on Numerical Weather Prediction, Amer. Meteor. Soc., J99-J102.

Proctor, F.H., and R.L. Bowles, 1992: Three-dimensional simulation of the Denver 11 July 1988 microburst-producing storm. *Meteorol. and Atmos. Phys.,* ***49***, 107-124.

Proctor, F.H., E.M. Bracalente, S.D. Harrah, G.F. Switzer, and C.L. Britt, 1995: Simulation of the 1994 Charlotte microburst with look-ahead windshear radar. Preprints, 27th Conference on Radar Meteorology, Amer. Meteor. Soc., 530-532.

Targ, R., and R.L. Bowles, 1988: Investigation of airborne lidar for avoidance of windshear hazards. AIAA-88-4658, 9 pp.

Vicroy, D.D., 1992: Assessment of microburst models for downdraft estimation. *J. Aircraft,* ***29,*** 1043-1048.

Vicroy, D.D., 1994: Microburst vertical wind estimation from horizontal wind measurements. NASA TR-3460, 83 pp.

Whiteman, C.D., B. Xindi, and S. Zhong, 1997: Low-level jet climatology from enhanced rawinsonde observations at a site in the southern Great Plains. *J. Appl. Meteor.,* ***36****,* 1363-1376.

Wilson, J.W., R.D. Roberts, C. Kessinger, and J. McCarthy, 1984: Microburst wind structure and evaluation of Doppler radar for airport wind shear detection. *J. Climate Appl. Meteor.,* ***23***, 898-915.

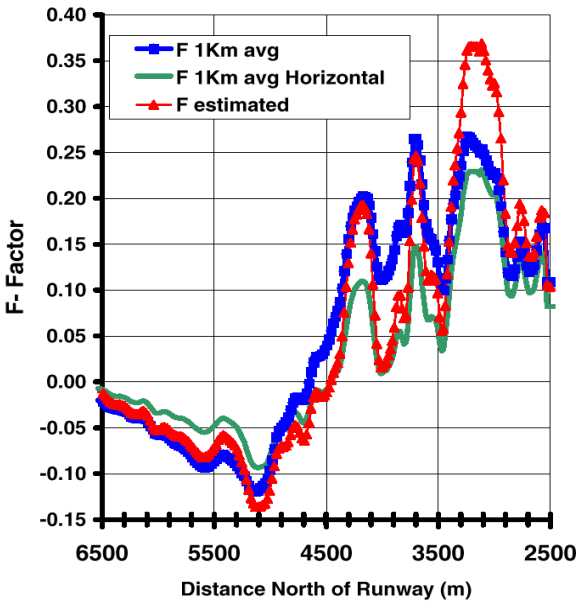

Figure 1. *Average F-factor experienced by Delta-191 during the 1985 DFW microburst encounter. The profile for estimated F is derived from Eq. (9).*

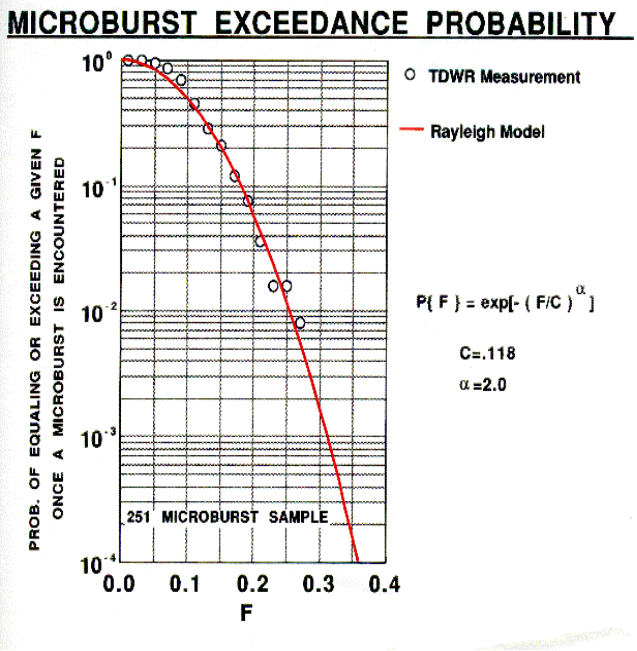

Figure 2. *Probability of a microburst exceeding a given* $\overline{F}$ **,** *based on a 251 microburst sample.*

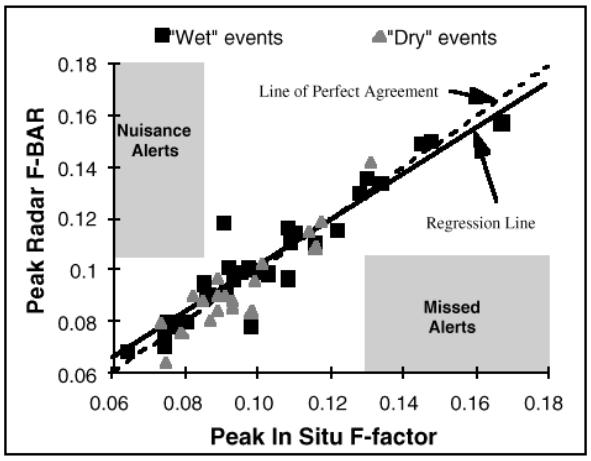

Figure 3. *Radar flight test performance (Bracalente et al 1994, Arbuckle et al 1996).*

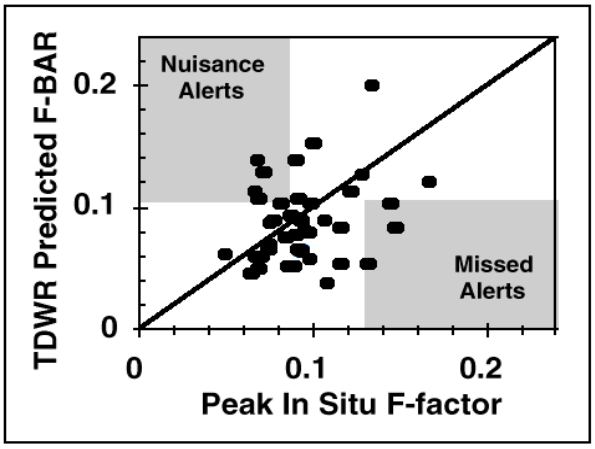

Figure 4. *TDWR vs in situ flight test performance (from Hinton 1993, 1994).*

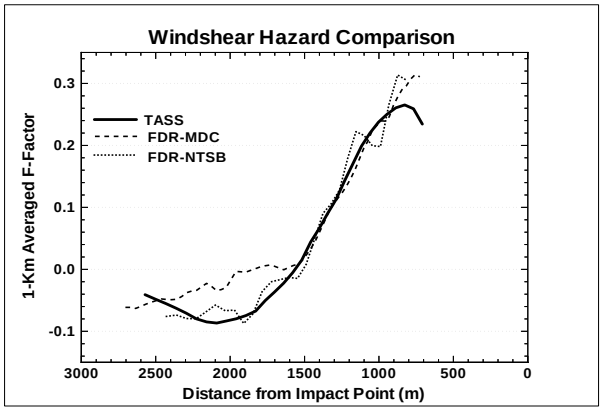

Figure 5 . *Comparison of reconstructed* $\overline{F}$ *profiles from the Charlotte windshear accident (Proctor et al 1995). Analyzed from numerical simulation (TASS) and FDR data. [The FDR data was obtained from two sources that differed slightly: McDonnell Douglas-MDC and NTSB].*

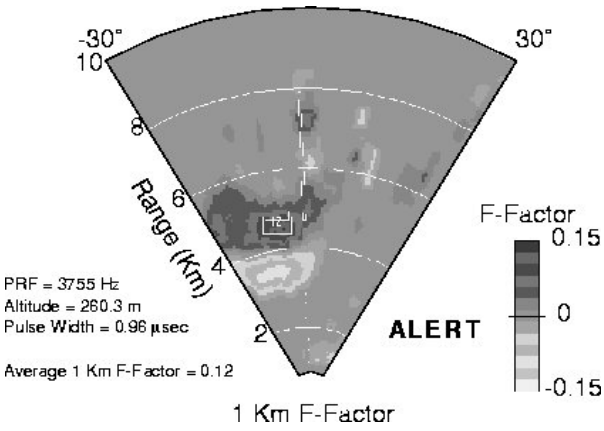

Figure 6. *Simulated windshear hazard as viewed by an onboard radar for the Charlotte accident (Proctor et al 1995). Viewed on approach 1 min prior to accident time.*